Pharmacogn. Mag.
A multifaceted peer reviewed journal in the field of Pharmacognosy and Natural Products
www.phcog.com | www.phcog.net

ORIGINAL ARTICLE

Docking-based Screening of *Ficus religiosa* Phytochemicals as Inhibitors of Human Histamine H2 Receptor

Amit Chaudhary, Birendra Singh Yadav, Swati Singh[1], Pramod Kumar Maurya, Alok Mishra, Shweta Srivastva, Pritish Kumar Varadwaj[2], Nand Kumar Singh, Ashutosh Mani

Department of Biotechnology, MNNIT, [1]Center of Bioinformatics, University of Allahabad, [2]Department of Applied Science, IIIT, Allahabad, Uttar Pradesh, India

Submitted: 08-02-2017 Revised: 21-03-2017 Published: 11-10-2017

ABSTRACT

Background: *Ficus religiosa* L. is generally known as Peepal and belongs to family *Moraceae*. The tree is a source of many compounds having high medicinal value. In gastrointestinal tract, histamine H2 receptors have key role in histamine-stimulated gastric acid secretion. Their over stimulation causes its excessive production which is responsible for gastric ulcer. **Objective:** This study aims to screen the range of phytochemicals present in *F. religiosa* for binding with human histamine H2 and identify therapeutics for a gastric ulcer from the plant. **Materials and Methods:** In this work, a 3D-structure of human histamine H2 receptor was modeled by using homology modeling and the predicted model was validated using PROCHECK. Docking studies were also performed to assess binding affinities between modeled receptor and 34 compounds. Molecular dynamics simulations were done to identify most stable receptor-ligand complexes. Absorption, distribution, metabolism, excretion, and screening was done to evaluate pharmacokinetic properties of compounds. **Results:** The results suggest that seven ligands, namely, germacrene, bergaptol, lanosterol, Ergost-5-en-3beta-ol, α-amyrin acetate, bergapten, and γ-cadinene showed better binding affinities. **Conclusion:** Among seven phytochemicals, lanosterol and α-amyrin acetate were found to have greater stability during simulation studies. These two compounds may be a suitable therapeutic agent against histamine H2 receptor.

Key words: Absorption, distribution, metabolism, excretion, and toxicity, docking, histamine H2 receptor, homology modeling, molecular dynamic simulation

SUMMARY

- This study was performed to screen antiulcer compounds from *F. religiosa*. Molecular modeling, molecular docking and MD simulation studies were performed with selected phytochemicals from *F. religiosa*. The analysis suggests that Lanosterol and α-amyrin may be a suitable therapeutic agent against histamine H2 receptor. This study facilitates initiation of the herbal drug discovery process for the antiulcer activity.

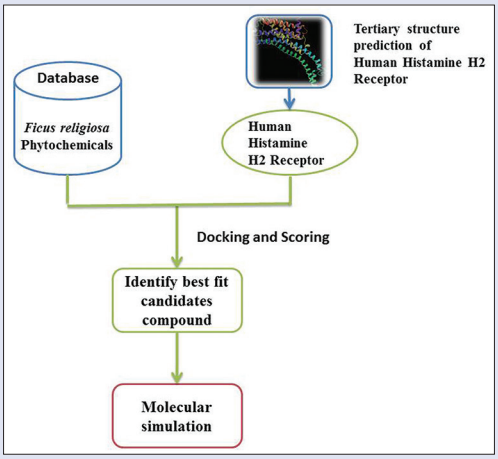

Abbreviations used: ADMET: Absorption, distribution, metabolism, excretion and toxicity, DOPE: Discrete Optimized Potential Energy, OPLS: Optimized potential for liquid simulations, RMSD: Root-mean-square deviation, HOA: Human oral absorption, MW: Molecular weight, SP: Standard-precision, XP: Extra-precision, GPCRs: G protein-coupled receptors, SASA: Solvent accessible surface area, Rg: Radius of gyration, NHB: Number of hydrogen bond

Correspondence:

Dr. Ashutosh Mani,
Department of Biotechnology,
MNNIT, Allahabad, Uttar Pradesh, India.
E-mail: ashutomani@gmail.com

DOI: 10.4103/pm.pm_49_17

Access this article online
Website: www.phcog.com
Quick Response Code:

INTRODUCTION

Herbs have been the important source of medicine in India since long. Medicinal plants have therapeutic properties due to the presence of various complex chemical substances of different compositions, which are formed as secondary plant metabolites in one or more parts of them. They are conventionally used due to their as therapeutic properties against diabetes,[1] cardiac diseases,[2] tuberculosis,[3] liver diseases,[4] asthma, cough-respiratory disorders,[5] and several other diseases.[6-13]

A peptic ulcer is a major cause of mortality in many countries. With the ever developing interest in natural medicine, many plants have been identified and reported to be useful in treating and managing ulcer. A peptic ulcer occurs in that part of the gastrointestinal tract which is unprotected to gastric acid and pepsin, i.e., the duodenum and stomach. The etiology of peptic ulcer is not clearly known. It probably occurs due to an imbalance between the aggressive (pepsin, acid, bile and *Helicobacter pylori*)[14] and the defensive (bicarbonate secretion and gastric mucus prostaglandins, nitric oxide innate resistance of the mucosal cells) factors.[15] An understanding of the control of gastric acid secretion and mechanism will elucidate the targets of antisecretory drug action.

Cite this article as: Chaudhary A, Yadav BS, Singh S, Maurya PK, Mishra A, Srivastva S, *et al*. Docking-based screening of *Ficus religiosa* phytochemicals as inhibitors of human histamine H2 receptor. Phcog Mag 2017;13:S706-14.

Histamine plays an important role in a variety of pathophysiological conditions. Histamine exerts its biological effects by binding to and activating four different separate rhodopsin-like G protein-coupled receptors-histamine H1, H2, H3, and H4. Each of the histamine receptors has a functional response, but their mechanism is different from each other.[16] Histamine H2 receptors primarily stimulate gastric acid secretion. H2 antagonists are also reported to be used in the clinical treatment of peptic ulceration.[17,18]

Ficus religiosa is a native Indian tree and commonly known as Peepal which belongs to the family *Moraceae*.[19] The preliminary phytochemical screening of different parts of *F. religiosa* plant such as bark, leaves, fruit, and seed has shown the presence of different chemicals of therapeutic value as shown in Table 1.[20-26] The studies on anti-ulcer (ulcer-preventive) effects of *F. religiosa* phytochemicals have shown positive results.[27-31]

In the current study, the structure of human histamine H2 receptor was modeled, molecular docking, and molecular dynamics (MD) simulation were performed between modeled histamine H2 receptor and *F. religiosa* phytochemicals. Phytochemicals were studied for their absorption, distribution, metabolism, excretion (ADME) properties. This work emphasizes on examining the binding interactions of human histamine H2 receptor with *F. religiosa* phytochemicals against gastric ulcer.

MATERIALS AND METHODS

Tertiary structure prediction

Molecular modeling of human histamine H2 receptor was performed using (Modeller 9.15) by homology modeling approach.[32] The sequence for the histamine H2 receptor isoform 2 (Homo sapiens) (Ref. Seq: NP_071640.1) was taken from database of NCBI.[33] The NCBI histamine H2 receptor sequence database contains protein sequences and their encoding regions derived from the nucleotide sequences. The sequence of histamine H2 receptor with GI: 13435405 were selected for three-dimensional (3D) model development that contains 359 amino acid residues with molecular weight 39967 Daltons. Suitable templates were searched with basic local alignment search tool against the Protein Databank.[34,35] On the basis of similarity search, four structures (2VT4, 2Y00, 4BVN, and 5A8E) from PDB were considered templates for modeling. Five 3D models were generated with different Discrete Optimized Potential Energy (DOPE)-scores featuring the accuracy of prediction [Figure 1]. Stereochemical quality of a protein structure and overall geometry was analyzed using PROCHECK server[36] and also produced a Ramachandran plot [Table 2 and Figure 2].

Ligand preparation

Ligprep was used for the preparation of ligands as shown in [Figure 3].[37] We obtained the initial ligand from PubChem database[38] and PDBchem in Structure Data Format. Without performing pre-docking filtering all structures were included and generated low energy 3D conformers with satisfactory bond lengths and angles for each two-dimensional structure. Optimized potential liquid simulation (OPLS2005) force field was used by Ligprep.[39] All possible protomers (protonation states) and ionization states were computed for the respective ligand using Ionizer at a pH

Table 1: List of phytochemicals in *Ficus religiosa*

Parts of plant	Phytochemicals	References
Bark	Lanosterol, bergapten, stigmasterol, bergaptol, β-sitosterol, lupen-3-one, β-sitosterol-d-glucoside (phytosterolin) Vitamin K1, wax	[20-22]
Leave	Stigmasterol, campestrol, isofucosterol, lupeol, tannic acid, serine, isoleucine, aspartic acid, glycine, threonine, alanine, proline, tryptophan, tryosine, methionine, valine leucine, n-nonacosane, n-hentricontanen, hexacosanol, n-octacosan	[23,24]
Fruit	Asgaragine, undecane, tetradecane, tridecane, (e)-β-ocimene, alloaromadendrene, α-thujeneβ-pinene, α-pinene, limonene, α-terpinene, dendrolasine, aromadendrene, dendrolasine α-ylangene, α- copaene, β-bourbonene, β-caryophyllene, α-trans bergamotene, α-humulene, germacrene, bicyclogermacrene, γ-cadinene, δ-cadinene	[25,26]
Seed	Alanine, tyrosine, threonine	[25]

Table 2: Ramachandran plot statistics for the predicted model (Seq.B99990003)

	Number of residues (%)
Most favored regions (A, B, L)	306 (92.7)
Additional allowed regions (a, b, l, p)	19 (5.8)
Generously allowed regions (~a, ~b, ~l, ~p)	2 (0.6)
Disallowed regions (XX)	3 (0.9)
Nonglycine and nonproline residues	330 (100.0)
End-residues (excl. Gly and Pro)	2
Glycine residues	16
Proline residues	11
Total number of residues	359

Based on an analysis of 118 structures of resolution of at least 2.0 Angstrom and R-factor no >20.0 a good quality model would be expected to have over 90% in the most favored regions (A, B, L)

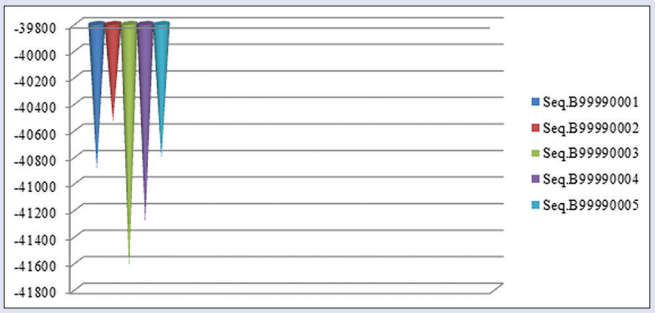

Figure 1: Graphical representation of Discrete Optimized Potential Energy score for Modeled structures

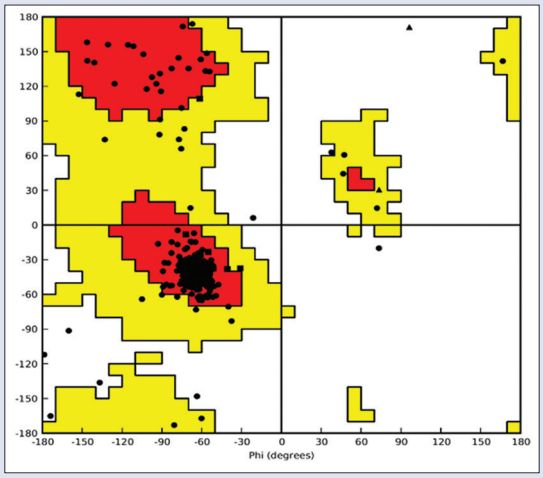

Figure 2: The classical Ramachandran or ϕ, ψ-plot (plotted for Seq. B99990003)

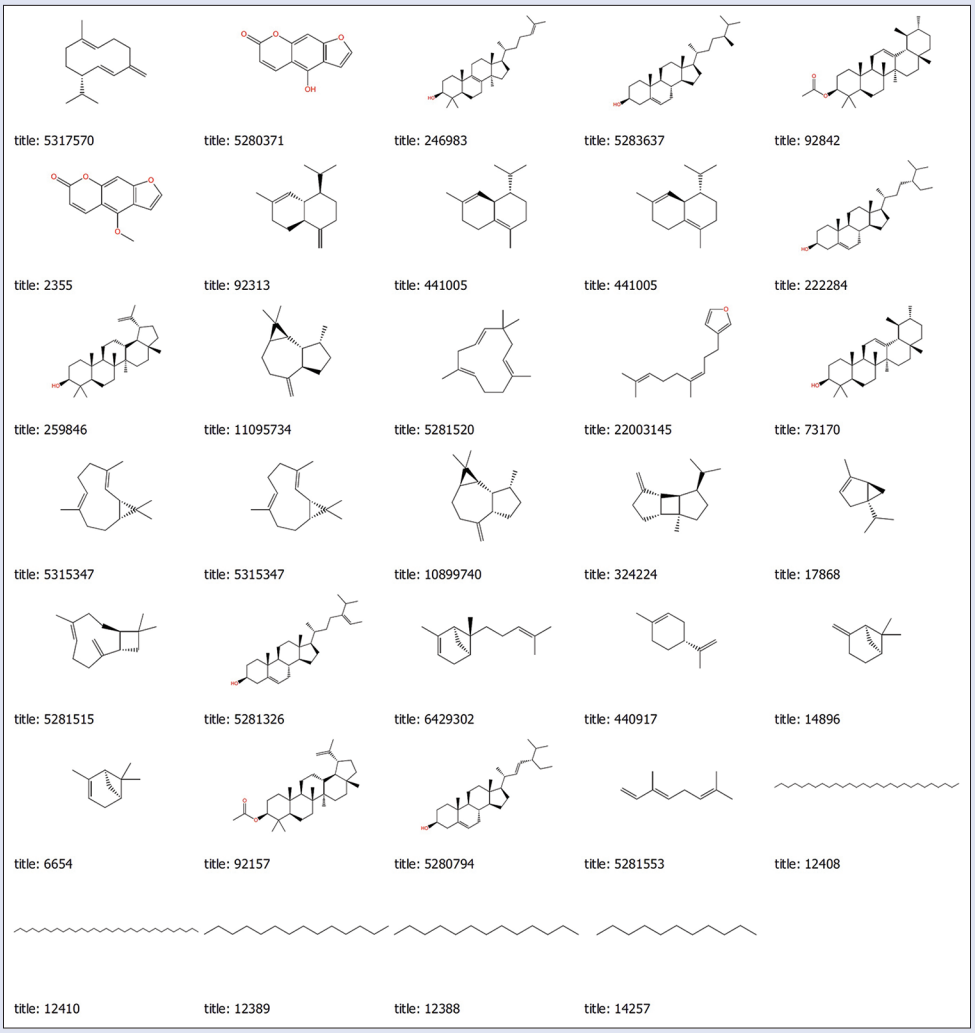

Figure 3: Chemical structure of ligands retrieved from PubChem

of 7.4. Tautomeric states were incorporated for chemical groups with possible prototropic, tautomerism. Only the lowest energy conformer was kept for all ligands.

Molecular docking of modeled protein with phytochemicals using GLIDE tool

Flexible docking was performed using Schrödinger software (New York, USA).[40] The docking calculations were performed using the Schrödinger software suite with default parameters and proteins were prepared using the Protein Preparation Wizard. Receptor grid was prepared with default parameters without any constraints.[40] SiteMap was used for prediction and evaluation of binding sites.[41] The emodel and glide scores were used to predict the binding affinity of docked structures using the SP and XP feature of GLIDE module implemented in the Schrödinger LLC.[42]

Functional assessment for absorption, distribution, metabolism, and excretion

QikProp v4.4 was used for ADME prediction program[43] which predicts physically significant descriptors and pharmaceutically related properties of organic molecules, either individually or in batches. Predicted significant ADME properties such as molecular weight (MW), donor hydrogen bond (HB), acceptor HB, QPlog, Po/w, % human oral absorption (HOA), the rule of five, central nervous system (CNS) were recorded. The predictions also included molecular properties, along with comparing a particular molecule's properties with those of 95% of known drugs.

Molecular dynamics simulations

Gromacs versions 5.1.2 was used to perform MD simulations for different protein-ligand complex.[44] The AMBER03 force field was used to generate the topologies for the complex.[45] Assigning of the protons to protein-ligand complex was performed automatically using the program pdb2 gmx within the GROMACS package. Complex systems were solvated with the TIP3P water model in a triclinic box under the periodic boundary conditions using a distance of 1.2 nm from the protein to the surface of the box. To neutralize the system, the number of counterions used for the complex was 54 NA and 69 CL ions, respectively. Each system was subjected to energy minimization using the steepest descent integrator without constraints for 2000 steps.[46] After minimization, systems were equilibrated under NVT (canonical ensemble) and NPT (isothermal–isobaric ensemble) conditions for 100 ps at 300 K after applying position restraints to the protein.[47] Finally, a 5000 ps production run was performed under NPT conditions by removing position restraints.

Berendsen weak-coupling method was used for maintaining temperature and pressure of the system.[48] Lennard-Jones potentials

were used for van der Waals interactions, and electrostatic interactions were handled by particle-mesh Ewald electrostatics calculations with a cut-off for the real space term of 0.8 nm.[49] The LINCS algorithm was used to constrain all the bonds.[50] A 2 fs time step was applied, and 2 ps final coordinates were saved. Most of the analyses for simulation studies were performed using Gromacs in-built tools such as root-mean-square deviation (RMSD), solvent-accessible surface area (SASA), a number of hydrogen bond (NHB), and radius of gyration (Rg) calculations were performed using a least-squares fit.[51] The production simulation was performed for 12 ns at 300 K. Xmgrace tool was used for graph plotting for all trajectory analysis.[52] The MD trajectories were analyzed using gmx_rmsd, gmx_SASA, gmx_NHB, and gmx_gyration of GROMACS utilities to get the RMSD, SASA of each system, the Rg and NHB.

RESULTS AND DISCUSSION

Prediction of histamine H2 receptor

The model (Seq.B99990003) of histamine H2 receptor isoform 2 (*Homo sapiens*) with the lowest DOPE score was selected for structure-based drug designing [Figure 4]. Stereo-chemical assessment of the predicted model shows that 92.7% of residues were in most favorable regions, 5.8% in allowed region, 0.6% in generously allowed regions, and 0.9% of the residues in disallowed regions [Table 3]. The selected protein models were found to be satisfactory for the calculated stereo-chemical parameters.

Docking of phytochemicals with histamine H2 receptor

Ligands were docked at the active site of the histamine H2 receptor which shows different respective docking score, Glide energy, Glide gscore, and Glide emodel [Table 4 and Figure 5]. The G-score and glide energy of the top seven ligands germacrene, bergaptol, lanosterol, Ergost-5-en-3beta-ol, α-amyrin acetate, bergapten, and γ-cadinene in the case of docking with histamine H2 receptor were found to be −5.838, −5.472, −5.423, −5.387, −5.255, −5.109, and −5.029, respectively [Table 5]. As well as the Glide-score, other parameters such as Glide energy, and the Glide E-model were also used for the evaluation of the docking results. Histamine H2 receptor complex has HB interactions between the ligand and the active site residues [Figures 6 and 7].

Table 3: Statistical potential for modeled structures

Name	DOPE score
Seq.B99990001	−40,908.570313
Seq.B99990002	−40,547.492188
Seq.B99990003	−41,647.273438
Seq.B99990004	−41,309.367188
Seq.B99990005	−40,825.726563

DOPE: Discrete Optimized Potential Energy

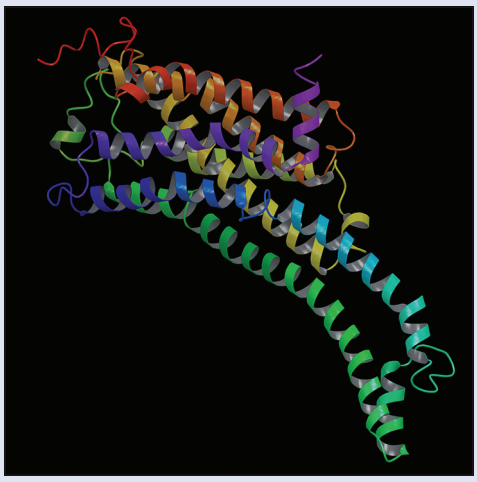

Figure 4: Three-dimensional representation of modeled histamine H2 receptor (Seq.B99990003)

Functional assessment for absorption, distribution, metabolism, excretion properties

About all descriptors and properties were reported of which few important are given in [Table 6]. The predicted values of MW, %HOA and permeability for all conformers were good [Figure 8a and b]. The drug-like activity of the ligand molecule is characterized using ADME properties and can be used to focus lead optimization efforts to enhance the desired properties of a given compound. Lanosterol and α-amyrin acetate hits displayed the properties such as MW, donor HB, acceptor HB, QPlog, Po/w, % HOA, the rule of five and CNS within the permissible range.

Molecular dynamics simulation

On the basis of lowest glide energy docked complex were selected for MD simulation. α-amyrin acetate-complex, lanosterol-complex, and Ergost-5-en-3beta-ol-complex showed lowest glide energy −33.358, −28.686 and −26.468, respectively. The RMSD for α-amyrin acetate-complex was found to be approximate 0.6 nm and it showed a gradual decrease after ~9000ps. α-amyrin acetate-complex maintained an overall stability throughout 12,000 ps of simulation, lanosterol-complex was found to be approximate 0.3 nm and it showed a gradual decrease after ~6000 ps. Lanosterol-complex maintained an overall stability throughout 12000 ps of simulation an Ergost-5-en-3beta-ol-complex was found to be approximately 0.9 nm and it showed a gradual increase after ~7000ps. Ergost-5-en-3beta-ol-complex showed more fluctuation in comparison to α-amyrin acetate-complex and lanosterol-complex [Figure 9].

The Rg was also calculated for the α-amyrin acetate-complex, lanosterol-complex, and Ergost-5-en-3beta-ol-complex to assess the compactness of the complex structure. The Rg range of the α-amyrin acetate-complex structure is between 2.8 and 2.95 nm. From 0 to ~6000 ps, there is a continuous decrease in the Rg value and further

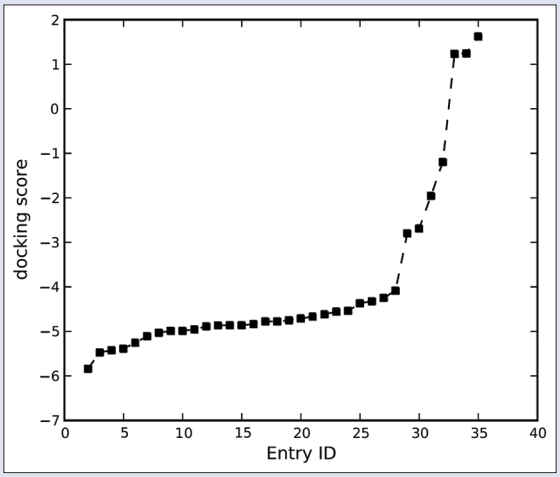

Figure 5: Docking score of protein with their corresponding entry IDs

Table 4: Inhibitory activity of phytochemicals on selected modeled structure

Compound's name	Entry ID	Docking score	Glide gscore	Glide energy	Glide emodel
Germacrene	Structure 3D_CID_5317570.1	−5.838	−5.838	−18.946	−25.386
Bergaptol	Structure 3D_CID_5280371.1	−5.472	−5.472	−25.178	−33.587
Lanosterol	Structure 3D_CID_246983.1	−5.423	−5.423	−28.686	−36.537
Ergost-5-en-3beta-ol	Structure 3D_CID_5283637.1	−5.387	−5.387	−26.468	−32.819
α-amyrin acetate	Structure 3D_CID_92842.1	−5.255	−5.255	−33.358	−43.441
Bergapten	Structure 3D_CID_2355.1	−5.109	−5.109	−24.886	−32.547
γ-cadinene	Structure 3D_CID_92313.1	−5.029	−5.029	−17.842	−23.148
δ-cadinene	Structure 3D_CID_441005.1	−4.988	−4.988	−18.788	−23.9
δ-cadinene	Structure 3D_CID_441005[1]	−4.988	−4.988	−18.788	−23.9
β-sitosterol	Structure 3D_CID_222284.1	−4.955	−4.955	−26.787	−33.491
Lupeol	Structure 3D_CID_259846.1	−4.885	−4.885	−31.989	−42.419
Aromadendrene	Structure 3D_CID_11095734.1	−4.865	−4.865	−20.933	−27.173
α-humulene	Structure 3D_CID_5281520.1	−4.861	−4.861	−21.946	−28.419
Dendrolasine	Structure 3D_CID_22003145.1	−4.861	−4.861	−23.571	−29.727
α-amyrin	Structure 3D_CID_73170.1	−4.836	−4.836	−31.706	−41.361
Bicyclogermacrene	Structure 3D_CID_5315347.1	−4.776	−4.776	−22.211	−28.615
Bicyclogermacrene	Structure 3D_CID_5315347[1]	−4.776	−4.776	−22.211	−28.615
Alloaromadendrene	Structure 3D_CID_10899740.1	−4.749	−4.749	−21.169	−27.223
β-bourbonene	Structure 3D_CID_324224.1	−4.711	−4.711	−17.241	−22.238
α-thujene	Structure 3D_CID_17868.1	−4.668	−4.668	−14.182	−18.462
β-caryophyllene	Structure 3D_CID_5281515.1	−4.617	−4.617	−18.828	−24.043
Isofucosterol	Structure 3D_CID_5281326.1	−4.557	−4.557	−24.115	−30.544
Bergamotene	Structure 3D_CID_6429302.1	−4.539	−4.539	−19.698	−25.17
Limonene	Structure 3D_CID_440917.1	−4.367	−4.367	−17.659	−21.979
β-pinene	Structure 3D_CID_14896.1	−4.324	−4.324	−15.468	−19.436
α-pinene	Structure 3D_CID_6654.1	−4.246	−4.246	−15.328	−19.234
Lupeol acetate	Structure 3D_CID_92157.1	−4.086	−4.086	−30.352	−38.569
Stigmasterol	Structure 2D_CID_5280794.1	−2.797	−2.797	−12.578	−11.753
β-ocimene	Structure 3D_CID_5281553.1	−2.691	−2.691	−14.96	−17.027
n-octacosan	Structure 2D_CID_12408.1	−1.957	−1.957	−20.49	−22.97
n-hentricontanen	Structure 2D_CID_12410.1	−1.197	−1.197	−10.166	−11.087
Tetradecane	Structure 3D_CID_12389.1	1.233	1.233	−20.714	−17.351
Tridecane	Structure 3D_CID_12388.1	1.245	1.245	−18.796	−16.019
Undecane	Structure 3D_CID_14257.1	1.622	1.622	−17.923	−14.047

Table 5: Docking analysis of histamine H2 receptor with top seven screened with interacting residues

Compound's name	Entry ID	Glide gscore	Interacting residues
Germacrene	Structure 3D_CID_5317570	−5.838	Leu141, Ile145, Leu107, Ile142, Phe110, Met111, Leu114, Phe56, Cys118, Ser138, Asp115
Bergaptol	Structure 3D_CID_5280371	−5.472	Cys118, Leu114, Tyr126, Asp115, Phe56, Met111, Ser138, Val130, Arg134, Leu129
Lanosterol	Structure 3D_CID_246983	−5.423	Val189, Pro194, Leu193, Leu107, Leu149, Ile145, Leu141, Ser138, Arg134, Val130, Val135, Tyr126, Leu52, Asp115, Phe56, Cys118, Met111, Leu114, Ile142, Phe110
Ergost-5-en-3beta-ol	Structure 3D_CID_5283637	−5.387	Ile145, Leu141, Ile142, Leu107, Pro194, Leu193, Ile197, Phe110, Leu114, Cys118, Asp115, Tyr126, Cys118, Arg134, Phe56, Ser138, Met111,
α-amyrin acetate	Structure 3D_CID_92842	−5.255	Leu107, Phe110, Met111, Ile142, Ile145, Leu141, Ser138, Phe56, Leu114, Asp115, Cys118, Tyr126, Val130, Arg134, Leu129, Arg125, Asp122
Bergapten	Structure 3D_CID_2355	−5.109	Cys118, Tyr126, Leu114, Asp115, Leu52, Val130, Ser138, Val135, Phe56, Met111, Arg134, Leu129
γ-cadinene	Structure 3D_CID_92313.1	−5.029	Arg134, Val135, Ile137, Leu141, Ile142, Phe110, Ser138, Met111, Leu114, Phe56, Asp115, Leu52, Val130, Tyr126

increased. Rg range of lanosterol-complex structure is between 2.73 and 2.93 nm. From 0 to ~6000 ps, there is a continuous increase in the Rg value and further decreased. Rg range of Ergost-5-en-3beta-ol-complex structure is between 2.65 to 2.86 nm. From 0ps to 12000ps obtained the Rg reduced [Figure 10].

The SASA was also calculated for the α-amyrin acetate-complex, lanosterol-complex and Ergost-5-en-3beta-ol. The SASA range of α-amyrin acetate-complex structure lies between 215 and 235 nm^2. The resulting α-amyrin acetate-complex showed a decrease in the SASA at ~6000 ps and then increased lanosterol-complex structure lies between 215 and 240 nm^2. The resulting lanosterol-complex showed an increase in the SASA at ~6000 ps and then decreased, and Ergost-5-en-3beta-ol-complex structure lies between 205 and 230 nm^2 and showed fluctuation increases and finally decreased [Figure 11]. The NHB of α-amyrin acetate-complex structure were obtained initially increased and after ~6000 ps reduced. The lanosterol-complex structure shows increased in number of HBs till 12,000 ps and Ergost-5-en-3beta-ol-complex structure showed decreased in the number of HB in comparison to α-amyrin acetate-complex and lanosterol-complex [Figure 12].

Herbal drugs are known to have minimal or no side effects. Peptic ulcer is a common problem in old as well as young people. Histamine stimulated gastric acid secretion is a normal phenomenon, but excessive stimulation causes increased acid production which

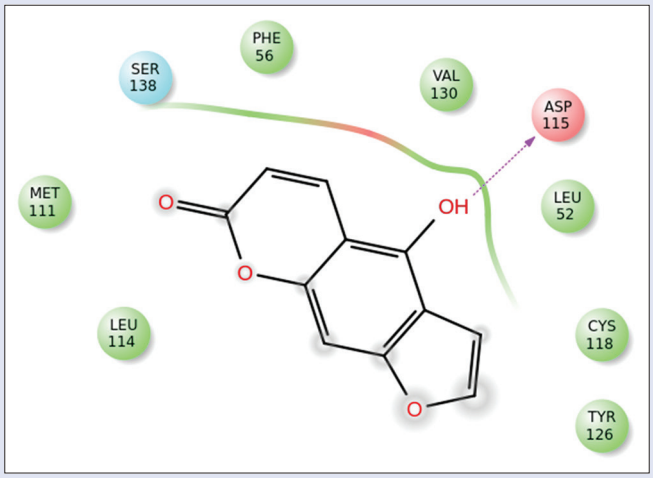

Figure 6: Schematic representations of ligand interactions with respective residues

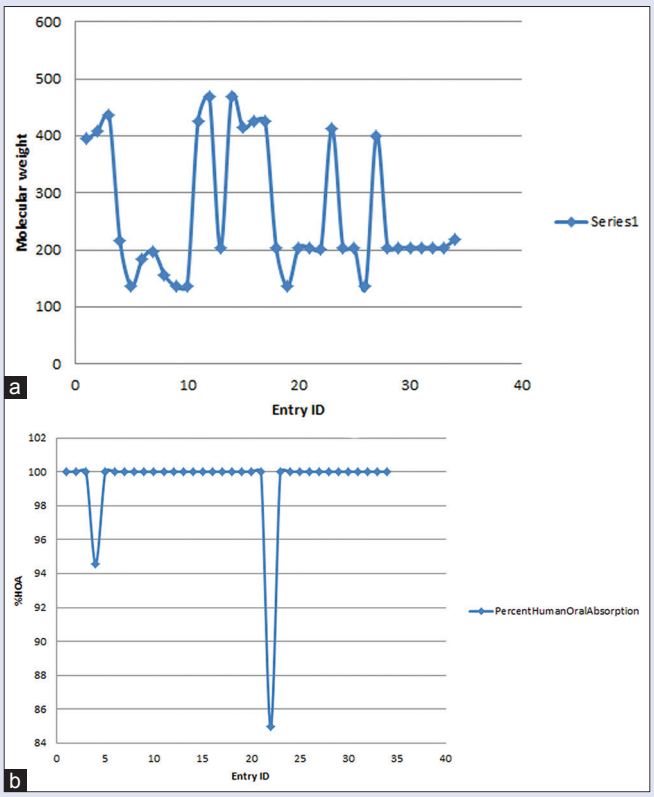

Figure 8: (a) Graphical representation of molecular weight with their respective entry IDs. (b) Graphical representation of % human oral absorption with their respective entry IDs

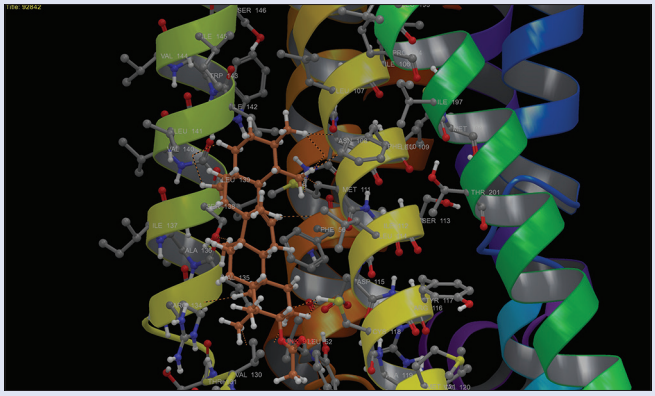

Figure 7: Human histamine H2 receptor in complex with α-amyrin acetate. Hydrogen bonds have been shown in yellow dashed line

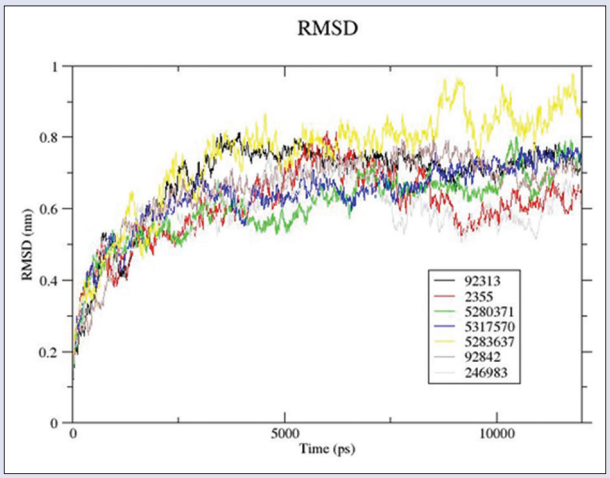

Figure 9: Root-mean-square deviation graphs of respective entry IDs (1) Structure3D_CID_92313, (2) Structure3D_CID_2355, (3) Structure3D_CID_5280371, (4) Structure3D_CID_5317570, (5) Structure3D_CID_5283637, (6) Structure3D_CID_92842, (7) Structure3D_CID_246983

contributes to peptic ulcer. Here, 34 compounds from *F. religiosa* were screened against the modeled structure of human histamine H2. Out of them, only seven compounds were found to have significantly high binding scores with the receptor. absorption, distribution, metabolism, excretion, and toxicity (ADMET) screening was done after docking to ensure that any highly promising prospective drug is not skipped only due to insignificant violation of pharmacokinetic properties. Stability of the receptor and ligand complexes were re-assessed using MD simulations. Trajectory, Rg and SASA analysis confirmed the docking results. Among seven phytochemicals lanosterol and α-amyrin acetate were found to have greater stability. In addition, they were also in accordance with the ADMET rules. Apart from screening, docking and MD simulation studies, the study helps in understanding the human histamine H2 and receptor interaction. The insights about the active site of the receptor will help in further analytics and investigations.

CONCLUSION

Molecular modeling, molecular docking and MD simulation studies were performed with selected phytochemicals from *F. religiosa*. The analysis suggests that lanosterol, α-amyrin acetate and Ergost-5-en-3beta-ol form the most stable complex with human histamine H2 receptor. The MD shows lanosterol and α-amyrin acetate have a relatively better binding affinity in comparison to others phytochemicals. Significantly both compounds satisfy all the *In silico* parameters such as docking score, glide energy, ADME/Tox and trajectories analysis. These two compounds may be a suitable therapeutic agent against histamine H2 receptor. This study facilitates initiation of the herbal drug discovery process for the antiulcer activity.

Table 6: Absorption, distribution, metabolism, excretion and toxicity properties of phytochemicals

PubChem CID	MW	Donor HB	Acceptor HB	QPlog Po/w	Percentage human oral absorption	Rule of five	CNS
12408	394.766	0	0	15.583	100	1	2
12409	408.793	0	0	16.051	100	1	2
12410	436.847	0	0	17.171	100	1	2
2355	216.193	0	3.75	1.429	94.591	0	0
6654	136.236	0	0	3.613	100	0	2
12388	184.364	0	0	7.812	100	1	2
12389	198.391	0	0	8.365	100	1	2
14257	156.311	0	0	6.701	100	1	2
14896	136.236	0	0	3.505	100	0	2
17868	136.236	0	0	3.836	100	0	2
73170	426.724	1	1.7	6.947	100	1	1
92157	468.762	0	2	7.866	100	1	1
92313	204.355	0	0	5.49	100	1	2
92842	468.762	0	2	8.056	100	1	1
222284	414.713	1	1.7	7.393	100	1	0
246983	426.724	1	1.7	7.523	100	1	0
259846	426.724	1	1.7	7.055	100	1	1
324224	204.355	0	0	5.115	100	1	2
440917	136.236	0	0	3.991	100	0	2
441005	204.355	0	0	5.489	100	1	2
441005	204.355	0	0	5.489	100	1	2
5280371	202.166	1	3.75	0.996	84.961	0	0
5281326	412.698	1	1.7	7.373	100	1	0
5281515	204.355	0	0	5.037	100	1	2
5281520	204.355	0	0	5.133	100	1	2
5281553	136.236	0	0	4.425	100	0	2
5283637	400.687	1	1.7	7.06	100	1	0
5315347	204.355	0	0	5.077	100	1	2
5315347	204.355	0	0	5.077	100	1	2
5317570	204.355	0	0	5.427	100	1	2
6429302	204.355	0	0	5.819	100	1	2
10899740	204.355	0	0	5.058	100	1	2
11095734	204.355	0	0	5.134	100	1	2
22003145	218.338	0	0.5	4.419	100	0	2

Permissible ranges for different parameters: Solute molecular weight (130.0/725.0); Donor HBs (0.0/6.0); Acceptor HBs (2.0/20.0); Percentage human oral absorption (±20%) (<25%: Poor), (>80%: High); Lipinski rule of 5 - (maximum=4); Predicted CNS activity (-- to ++) - −2 (inactive), +2 (active). QPlog Po/w: 2.0-6.5. QPlog Po/w: Predicted octanol/water partition coefficient; CNS: Central nervous system; HBs: Hydrogen bonds; MW: Molecular weight; +: CNS-active; -:CNS-inactive

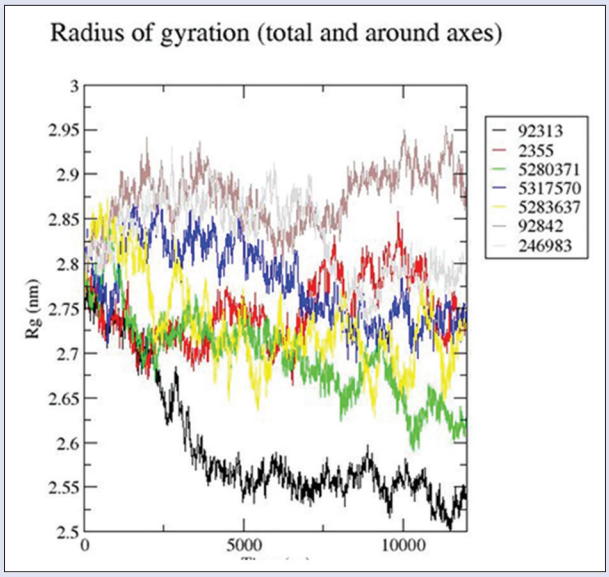

Figure 10: Rg graphs of respective entry IDs (1) Structure3D_CID_92313, (2) Structure3D_CID_2355, (3) Structure3D_CID_5280371, (4) Structure3D_CID_5317570, (5) Structure3D_CID_5283637, (6) Structure3D_CID_92842, (7) Structure3D_CID_246983

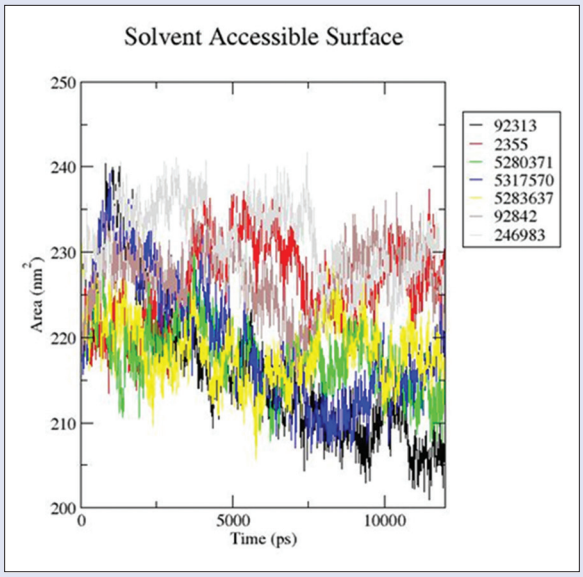

Figure 11: Solvent accessible surface area graphs of respective entry IDs (1) Structure3D_CID_92313, (2) Structure3D_CID_2355, (3) Structure3D_CID_5280371, (4) Structure3D_CID_5317570, (5) Structure3D_CID_5283637, (6) Structure3D_CID_92842, (7) Structure3D_CID_246983

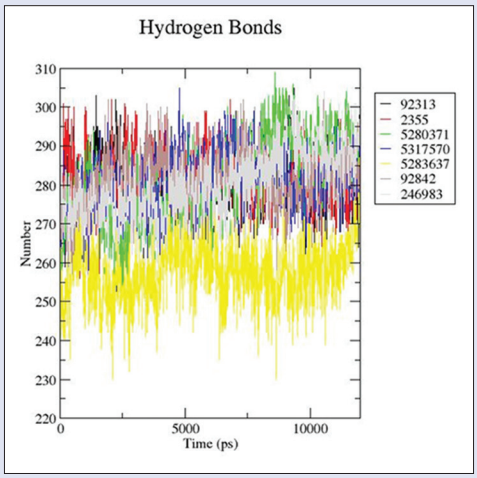

Figure 12: Number of hydrogen bond graphs of respective entry IDs (1) Structure3D_CID_92313, (2) Structure3D_CID_2355, (3) Structure3D_CID_5280371, (4) Structure3D_CID_5317570, (5) Structure3D_CID_5283637, (6) Structure3D_CID_92842, (7) Structure3D_CID_246983

Acknowledgement

The authors are thankful to the Department of Biotechnology, MNNIT-Allahabad for providing essential facilities. Computing facility availed at IIIT Allahabad is highly acknowledged.

Financial support and sponsorship

AC and PKM are thankful to MNNIT Allahabad for PhD fellowship.

Conflicts of interest

There are no conflicts of interest.

REFERENCES

1. Brahmachari HD, Augusti KT. Orally effective hypoglycemic agents from plants. J Pharm Pharmacol 1962;14:254-5.
2. Kirtikar KR, Basu BD. Indian Medicinal Plants. 2nd ed., Vol. III. New Delhi, India: Periodical Experts Book Agency; 1993. p. 2317-9.
3. Khanom F, Kayahara H, Tadasa K. Superoxide-scavenging and prolyl endopeptidase inhibitory activities of Bangladeshi indigenous medicinal plants. Biosci Biotechnol Biochem 2000;64:837-40.
4. Kotoky J, Das PN. Medicinal plants used for liver diseases in some parts of Kamrup district of Assam, a North Eastern State of India. Fitoterapia 2008;79:384-7.
5. Mahishi P, Srinivasa BH, Shivanna MB. Medicinal plant wealth of local communities in some villages in Shimoga District of Karnataka, India. J Ethnopharmacol 2005;98:307-12.
6. Rout SD, Panda T, Mishra N. Ethno-medicinal plants used to cure different diseases by tribals of Mayurbhanj district of North Orissa. Stud Ethno Med 2009;3:27-2.
7. Williamson EM, Hooper PM. Major Herbs of Ayurveda. London: Churchill Livingstone; 2002. p. 145-9.
8. Poonam K, Singh GS. Ethnobotanical study of medicinal plants used by the Taungya community in Terai Arc Landscape, India. J Ethnopharmacol 2009;123:167-76.
9. Lansky EP, Paavilainen HM, Pawlus AD, Newman RA. *Ficus* spp. (fig): Ethnobotany and potential as anticancer and anti-inflammatory agents. J Ethnopharmacol 2008;119:195-213.
10. Kirana H, Agrawal SS, Srinivasan BP. Aqueous extract of *Ficus religiosa* linn. reduces oxidative stress in experimentally induced type 2 diabetic rats. Indian J Exp Biol 2009;47:822-6.
11. Balachandran P, Govindarajan R. Cancer – an ayurvedic perspective. Pharmacol Res 2005;51:19-30.
12. Warrier PK, Nambiar VP, Ramankutty C. Indian Medicinal Plants: A Compendium of 500 Species. Vol. III. Chennai: Orient Longman Pvt. Ltd; 1995. p. 38-42.
13. Jain A, Katewa SS, Chaudhary BL, Galav P. Folk herbal medicines used in birth control and sexual diseases by tribals of southern Rajasthan, India. J Ethnopharmacol 2004;90:171-7.
14. Dale MM, Rang HP, Dale MM. Rang and Dale's Pharmacology. Edinburgh: Churchill Livingstone; 2007.
15. Tripathi KD. Essentials of Medical Pharmacology. New Delhi: Jaypee Brothers, JP Medical Ltd.; 2013.
16. Hill SJ, Ganellin CR, Timmerman H, Schwartz JC, Shankley NP, Young JM, *et al.* International union of pharmacology. XIII. Classification of histamine receptors. Pharmacol Rev 1997;49:253-78.
17. Code CF. Histamine and gastric secretion. In: Ciba Foundation Symposium-Histamine. Chichester, UK: John Wiley and Sons, Ltd.; 1956. p. 189-9.
18. Cooper DG, Young RC, Durant GJ, Ganellin CR. Histamine receptors. Compr Med Chem 1990;3:323-1.
19. Chandrasekar SB, Bhanumathy M, Pawar AT, Somasundaram T. Phytopharmacology of *Ficus religiosa*. Pharmacogn Rev 2010;4:195-9.
20. Rajiv P, Sivaraj R. Screening for phytochemicals and antimicrobial activit of aqueous extract of *Ficus religiosa* Linn. Int J Pharm Pharm Sci 2012;4:207-9.
21. Ambika SH, Rao MR. Studies on a phytosteroin from the bark of *Ficus religiosa*. Indian J Pharm 1967;29:91-4.
22. Swami KD, Bisht NP. Constituents of *Ficus religiosa* and *Ficus infectoria* and their biological activity. J Indian Chem Soc 1996;73:631.
23. Behari M, Rani KU, Matsumoto T, Shimizu N. Isolation of active-principles from the leaves of *Ficus religiosa*. Curr Agric 1984;8:73-6.
24. Verma RS, Bhatia KS. Chromatographic study of amino acids of the leaf protein concentrates of *Ficus religiosa* Linn and *Mimusops elengi* Linn. Indian J Hosp Pharm 1986;23:231-2.
25. Ali M, Qadry JS. Amino acid composition of fruits and seeds of medicinal plants. J Indian Chem Soc 1987;64:230-1.
26. Mali S, Borges RM. Phenolics, fibre, alkaloids, saponins, and cyanogenic glycosides in a seasonal cloud forest in India. Biochem Syst Ecol 2003;31:1221-6.
27. Saha S, Goswami G. Study of antiulcer activity of *Ficus religiosa* L. on experimentally induced gastric ulcers in rats. Asian Pac J Trop Med 2010;3:791-3.
28. Bansal VK, Goyal SK, Goswami DS, Singla S, Rahar S, Kumar S. Herbal approach to peptic ulcer disease: Review. J Biosci Tech 2009;1:52-8.
29. Feldman M, Burton ME. Histamine2-receptor antagonists. Standard therapy for acid-peptic diseases 1. N Engl J Med 1990;323:1672-80.
30. Parsons ME, Ganellin CR. Histamine and its receptors. Br J Pharmacol 2006;147 Suppl 1:S127-35.
31. Hirschowitz BI. H-2 histamine receptors. Annu Rev Pharmacol Toxicol 1979;19:203-4.
32. Webb B, Sali A. Comparative Protein Structure Modeling Using MODELLER. Curr Protoc Bioinformatics 2014;47:5.6:5.6.1–5.6.32.
33. Schmutz J, Martin J, Terry A, Couronne O, Grimwood J, Lowry S, *et al.* The DNA sequence and comparative analysis of human chromosome 5. Nature 2004;431:268-274.
34. Berman HM, Westbrook J, Feng Z, Gilliland G, Bhat TN, Weissig H, *et al.* The Protein Data Bank. Nucleic Acids Research 2000;28:235-42.
35. Altschul SF, Gish W, Miller W, Myers EW, Lipman DJ. Basic local alignment search tool. J Mol Biol 1990;215:403-10.
36. Laskowski RA, MacArthur MW, Moss DS, Thornton JM. PROCHECK: A program to check the stereochemical quality of protein structures. J Appl Crystallogr 1993;26:283-1.
37. LigPrep. Ver. 2.3. New York: Schrödinger, LLC,; 2009.
38. Bolton EE, Wang Y, Thiessen PA, Bryant SH. PubChem: Integrated platform of small molecules and biological activities. Ann Rep Comput Chem 2008;4:217-1.
39. Sastry GM, Adzhigirey M, Day T, Annabhimoju R, Sherman W. Protein and ligand preparation: Parameters, protocols, and influence on virtual screening enrichments. J Comput Aided Mol Des 2013;27:221-34.
40. Dinesh KB, Vignesh KP, Bhuvaneshwaran, SP, Mitra A. Advanced drug designing softwares and their applications in medical research. Int J Pharm Pharm Sci 2010;2:16-8.
41. Halgren T. New method for fast and accurate binding-site identification and analysis. Chem Biol Drug Des 2007;69:146-8.
42. Friesner RA, Banks JL, Murphy RB, Halgren TA, Klicic JJ, Mainz DT, *et al.* Glide: A new approach for rapid, accurate docking and scoring 1. Method and assessment of docking accuracy. J Med Chem 2004;47:1739-49.
43. Schrödinger Release 2015-2: LigPrep version 2.3. New York, NY: Schrödinger, LLC; 2015.
44. Abraham MJ, van der Spoel D, Lindahl E, Hess B. GROMACS User Manual. Ver. 5.1. 2. KTH (Royal Technical Institute), Stockholm: The GROMACS Development Team; 2016.

45. Cordomí A, Caltabiano G, Pardo L. Membrane protein simulations using AMBER force field and berger lipid parameters. J Chem Theory Comput 2012;8:948-58.
46. Hirshman SP, Whitson JC. Steepest-descent moment method for three-dimensional magnetohydrodynamic equilibria. Phys Fluids 1983;26:3553-8.
47. Andersen HC. Molecular dynamics simulations at constant pressure and/or temperature. J Chem Phy 1980;72:2384-3.
48. Van Der Spoel D, Lindahl E, Hess B, Groenhof G, Mark AE, Berendsen HJ. GROMACS: Fast, flexible, and free. J Comput Chem 2005;26:1701-18.
49. Cheatham TI, Miller JL, Fox T, Darden TA, Kollman PA. Molecular dynamics simulations on solvated biomolecular systems: the particle mesh Ewald method leads to stable trajectories of DNA, RNA, and proteins. Journal of the American Chemical Society 1995;117:4193-4.
50. Hess B, Bekker H, Berendsen HJ, Fraaije JG. LINCS: A linear constraint solver for molecular simulations. J Comput Chem 1997;18:1463-2.
51. Lindahl E, Hess B, Van Der Spoel D. GROMACS 3.0: A package for molecular simulation and trajectory analysis. J Mol Model 2001;8:306-17.
52. Turner PJ. XMGRACE Version 5.1.19. Beaverton, ORE, USA: Central for costal and Land-Margin Research; Oregon Graduate Institute of Science and Technology; 2005.